Molecular Mass Dependence of Interfacial Tension in Complex Coacervation

Debra J. Audus,[1,*] Samim Ali,[1,†] Artem M. Rumyantsev,[2] Yuanchi Ma,[1] Juan J. de Pablo,[2,‡] and Vivek M. Prabhu[1]
[1]Materials Science and Engineering Division, National Institute of Standards and Technology, Gaithersburg, Maryland 20899, USA
[2]Pritzker School of Molecular Engineering, University of Chicago, Chicago, Illinois 60637, USA

(Received 7 December 2020; revised 19 February 2021; accepted 16 April 2021; published 11 June 2021)

The interfacial tension of coacervates, the liquidlike phase composed of oppositely charged polymers that coexists at equilibrium with a supernatant, forms the basis for multiple technologies. Here we present a comprehensive set of experiments and molecular dynamics simulations to probe the effect of molecular mass on interfacial tension γ, far from the critical point, and derive $\gamma = \gamma_\infty(1 - h/N)$, where N is the degree of polymerization, γ_∞ is the infinite molecular mass limit, and h is a constant that physically corresponds to the number of monomers of one chain within the coacervate correlation volume.

DOI: 10.1103/PhysRevLett.126.237801

Under suitable conditions, solutions of oppositely charged polymers can form a liquidlike complex coacervate phase in coexistence with a supernatant phase—a phenomenon known as complex coacervation [1–6]. A key feature of these coacervates is their ultralow interfacial tension [7–10] making them appealing for a variety of applications including underwater adhesives [11], biomedical technologies [12], etc. [2–4]. Ultralow interfacial tension is also an important property in biological systems such as membraneless organelles [13], which have been described as coacervates [14–16]. However, the full functional dependence of the interfacial tension on all relevant quantities—salt, temperature, molecular mass—in all regimes is not yet known. This is in direct contrast with neutral systems, where extensive efforts have led to a comprehensive characterization of the interfacial tension and interfacial profiles, including the effects of polydispersity [17–22].

Most work thus far has focused on the salt dependence, as the addition of salt can act as a stimulus shifting the two-phase system to a homogeneous solution. There have been several experiments [7–9], simulations [23,24], and, most notably, a derivation [25] of scaling laws using the Voorn-Overbeek theory [26,27] coupled with the Cahn-Hilliard theory [28]. Specifically, Qin and co-workers found that the interfacial tension γ goes as $(1 - \psi/\psi_{cr})^{3/2}/N^{1/4}$ near the critical point where ψ is the salt concentration, ψ_{cr} is the critical salt concentration and N is the degree of polymerization.

Qin and co-workers derived the dependence of the interfacial tension on degree of polymerization—the most important nonstimuli design parameter—near the critical point. The behavior far from the critical point, however, is still unknown. In the context of coacervate-based applications, this knowledge is essential for informed design. For underwater adhesives, the initial formulation should offer good wettability and be far from the critical point, such that stimuli such as pH can trigger a phase transition to a precipitate or gel phase [29]. For encapsulation, droplet size depends on the surface tension, and being far from the critical point enables a dramatic enrichment of cargo such as RNA, proteins, or flavor-enhancing molecules [12].

The lack of theory in this regime is partly due to a scarcity of experimental data to motivate a derivation. To date, only one study by Priftis and co-workers [8] has explored the molecular mass dependence. They considered three molecular masses of poly(L-glutamic acid sodium salt) and poly(L-lysine hydrochloride). As one measurement was likely close to the critical point, only two points were left to ascertain the trend of molecular mass far from the critical point. In this Letter, we fill this gap in the literature by performing experimental measurements for the molecular mass dependence far from the critical point. We derive this dependence and further validate it via molecular dynamics simulations. The resulting interfacial profiles are computed and compared to theory.

In order to experimentally measure the interfacial tension for different molecular masses, several key elements are needed: a reliable method for measuring ultralow interfacial tensions, low-polydispersity polymers, and a series of different molecular mass model polymers that form coacervates at the same salt concentration.

We mix polyacrylic acid (PAA) and quaternized poly (dimethyl aminoethyl methacrylate) (qPDMAEMA) [30] of varying molecular masses at a 1:1 charge stoichiometric ratio in water at an initial polymer concentration of 0.3 mol/L. After trial and error, it was determined that the measurement criteria were satisfied over a wide degree of polymerization ($69 < N < 451$) and temperature (stable down to 0 °C) when the salt (NaCl) concentration is 100 mmol/L and the pH is 6.5. To confirm these findings, we also measured the concentration in both the supernatant

TABLE I. Experimental data for total polymer concentrations (c_p) and interfacial tension (γ). $1/N^* = 1/(2N_{\mathrm{PAA}}) + 1/(2N_{\mathrm{qPDMAEMA}})$ for consistency with Ref. [19].

N^*	c_p (Supernatant) (mol/L)	c_p (Coacervate) (mol/L)	γ (μN/m)
69.5	0.0058 ± 0.0009	3.24 ± 0.1	180 ± 18
145.0	0	3.46 ± 0.11	610 ± 50
218.9	0	3.27 ± 0.11	750 ± 69
485.6	0.001 ± 0.004	3.36 ± 0.11	880 ± 57

and the coacervate (see Supplemental Material [31] for details). As can be seen in Table I, the concentrations in both phases confirm that the system is far from the critical point.

To robustly measure ultralow interfacial tension, we leverage recent work by Ali and co-workers that combined deformed drop retraction analysis and the lower critical solution temperature property of complex coacervates [9,37]. Coacervate, in contact with its supernatant, is placed in a 500 to 800 μm gap between the parallel plates of a shear cell. After a temperature jump and subsequent equilibration at 25 °C, well separated 30 to 150 μm drops of dilute (supernatant) phase are formed. These spherical drops are deformed to an ellipsoidal shape by applying a deforming strain controlled via the shear plate. After the deforming strain is withdrawn, the retraction of the drop to a spherical shape is measured. This information, combined with the zero-shear viscosity of the coacervate and supernatant, enables quantification of the interfacial tension. Additional experimental details including the necessary rheological analysis and equations for time-dependent droplet shape analysis are provided in the Supplemental Material [31]. The results of these measurements are in Table I and Fig. 1. The error bars for the interfacial tension are obtained from 1 standard deviation in the retraction times measured for at least seven independent drops of varying sizes.

Empirically, we find that

$$\gamma = \gamma_\infty (1 - h/N), \tag{1}$$

(the black line in Fig. 1), where γ_∞ is the interfacial tension for infinite molecular mass and h is a constant that is dependent on the system and its conditions (temperature, charge density, etc.). In order to understand this behavior from a theoretical perspective, we start with two key assumptions: (i) the only N dependence in the free energy is contained in the ideal gas term and (ii) the system is far from the critical point, where the concentration of the polymer in the supernatant phase can be approximated as zero. The first assumption is in line with a variety of existing theories not only for complex coacervates

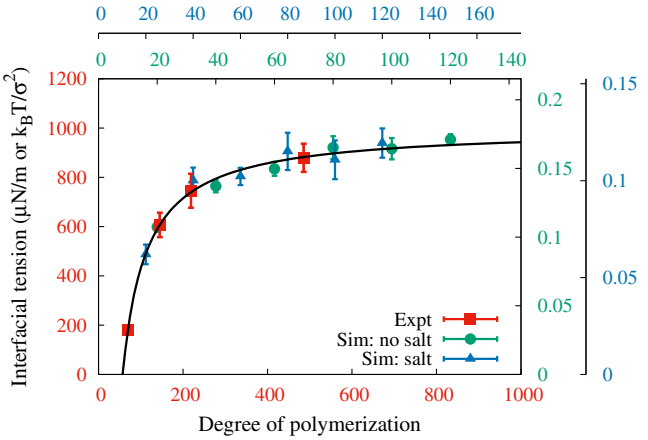

FIG. 1. Interfacial tension as a function of the degree of polymerization for the experimental system of PAA and qPDMAEMA, as well as molecular dynamics of coarse-grained polymers in a theta solvent both with and without salt. In all cases, the functional form for the data is $\gamma = \gamma_\infty(1 - h/N)$. For the experimental data, $\gamma_\infty = 999.6 \pm 3.5$ μN/m, $h = 56.97 \pm 0.11$, and N^* is used for the degree of polymerization (see Table I). Uncertainty in the fit represents standard error.

[26,38–41], but also for polymeric systems in general [42–44]. The second assumption is found to be true within the uncertainty of our measurements (see Table I) and is consistent with prior experiments [45,46] and simulations [41] where the concentration in the supernatant was found to be 2 to 3 orders of magnitude smaller than that of the coacervate.

We initially ignore the counterions and salt and relax this constraint later. The dimensionless free energy density is

$$f = \frac{\phi}{N} \ln \phi + g(\phi), \tag{2}$$

where ϕ is the monomeric density and $g(\phi)$ can take any physically realistic form.

To provide physical intuition, we consider the free energy of complex coacervation for polymers in a theta solvent, with the electrostatics treated using the random phase (one-loop) approximation that accounts for connectivity of charges in polymers [38,39,47]. Namely,

$$g(\phi) = w\phi^3 + \alpha^{3/4}\phi^{3/4}. \tag{3}$$

$2w$ is the third virial coefficient and $\alpha \equiv 12\pi \ell_B \sigma_c^2 / [(3\pi)^{4/3} b^2]$ where ℓ_B is the Bjerrum length, which measures the length scale at which the electrostatic energy is 1 $k_B T$, σ_c is the fraction of charged monomers, and b is the Kuhn length. Although this theory is only strictly valid for low charge densities, unlike the experimental system considered here, it allows for determination of γ_∞ and h, as well as calculation of interfacial profiles.

Prior to determining the interfacial tension, we determine the coacervate concentration by assuming the polymer concentration to be negligible in the supernatant, and solving for equal osmotic pressures in both phases [$\Pi = \phi f'(\phi) - f(\phi) = 0$]. Applying a perturbative analysis [48] on ϕ yields an expansion in powers of $1/N$:

$$\phi = \phi_\infty - \frac{a}{N} + \mathcal{O}\left(\frac{1}{N^2}\right), \tag{4}$$

where ϕ_∞ and a are subject to

$$\phi_\infty g'(\phi_\infty) - g(\phi_\infty) = 0 \tag{5}$$

and

$$a = 1/g''(\phi_\infty). \tag{6}$$

As $g(\phi_\infty)$ is convex, a is positive.

For the analytic theta solvent case [see Eq. (3)],

$$\phi = \frac{\alpha^{1/3}}{(8w)^{4/9}} - \frac{2^{7/3}}{9w^{5/9}\alpha^{1/3}N} + \mathcal{O}\left(\frac{1}{N^2}\right), \tag{7}$$

which recovers the expression derived above in the limit that N approaches infinity [47,49–51].

To confirm this expansion numerically, we perform molecular dynamics simulations of coarse-grained polymers [52] using the Lennard-Jones potential with a well depth of 0.3 in reduced units and a cutoff of 2.5σ, where σ is the bead diameter, to mimic a theta solvent [53]. Each bead has a unit charge, and the dielectric constant is 1 in reduced units (in the weak association regime; see Ref. [54]). A particle-particle particle-mesh Ewald scheme with an accuracy of 10^4, an order of 5, and an electrostatic cutoff of 5σ is used. No counterions or salt are included. The simulation box is 35σ by 35σ by 350σ. Simulations are initialized using a self-avoiding random walk of polymers in a cubic box of 35σ with a density of $0.5\sigma^{-3}$ close to the final density. A timestep of 0.005, and a total of 9×10^6 steps are used for production after an equilibration of 10^6 steps. The lengthy production run combined with a large box size is required to achieve good statistics as the fluctuations in the interfacial tension are large. Equilibration is monitored both through end-to-end distance of the polymers and interfacial tension. Error bars are determined from the standard deviation of the five replicates. All simulations are performed using the Large-scale Atomic/Molecular Massively Parallel Simulator (LAMMPS) [55,56].

The resulting concentration as a function of N is plotted in Fig. 2. The data can be successfully fit using the derived functional form [Eq. (4)]. Interestingly, ignoring higher order terms works well, even down to small values of N. The experimental data (see Table I) can also be fit with the

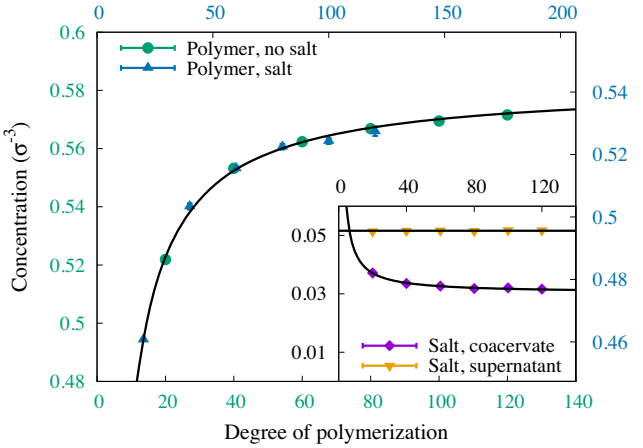

FIG. 2. Polymer concentration in the coacervate phase both with and without salt, as well as salt concentration in both phases as a function of the degree of polymerization for coarse-grained polymers in a theta solvent. Most error bars are smaller than the symbol size.

derived functional form (see Fig. S3 [31]); however, we opted not to plot it in Fig. 2 as it can also be fit to $c_p = c_{p,\infty}$ as $a = 0$ within uncertainty.

Using Cahn-Hilliard theory [28], the interfacial tension can be written as

$$\gamma = 2\int_0^{\phi_c} [\kappa \Delta f]^{1/2} d\phi. \tag{8}$$

Here ϕ_c is the monomeric concentration in the coacervate phase, κ is the square gradient term and is equal to $b^2/(24\phi)$ [42,57,58], while Δf is the free energy per volume for transferring a polymer from an infinite reservoir of ϕ_c to ϕ and is equal to $f(\phi) - \phi f'(\phi_c)$ [28,59].

After mathematical manipulation (see Supplemental Material [31] for details), one finds Eq. (1) with

$$\gamma_\infty = \frac{\phi_\infty^{1/2} b}{\sqrt{6}} \int_0^1 A^{1/2}(\phi_\infty, \eta) d\eta \tag{9}$$

and

$$h = -\frac{\int_0^1 \frac{\phi_\infty \ln \eta}{2\sqrt{A(\phi_\infty,\eta)}} d\eta}{\int_0^1 \sqrt{A(\phi_\infty,\eta)} d\eta}, \tag{10}$$

where $\eta \equiv \phi/\phi_c$ and $A(\phi_\infty, \eta) = g(\eta\phi_\infty)/\eta - g(\phi_\infty)$. As η must be less than or equal to one, h is positive; h has no dependence on a because terms that are of $\mathcal{O}(1/N)$ in the expression for h are equivalent to terms that are of $\mathcal{O}(1/N^2)$ in γ, and thus can be ignored.

For the analytic theta solvent case

$$\gamma_\infty = 0.070 b \alpha^{2/3} w^{-7/18} \tag{11}$$

and

$$h = 2.4\alpha^{-2/3}w^{-1/9}. \tag{12}$$

The expression for γ_∞ recovers previously derived expressions [47,49,50], and the equation for h scales as the number of monomers within the coacervate correlation volume ($\xi^2 \simeq \phi\xi^3$ for $w \simeq 1$, where ξ is the correlation length). See Eqs. (8) and (9) in Ref. [47]. For coacervates of low density, $\phi \ll 1$, this physical meaning of h is general and independent of the particular form of $g(\phi)$, as demonstrated in the Supplemental Material [31].

To further test the theory, we can calculate the interfacial tension from the simulations using the pressure tensor [via the first line of Eq. (24) in Ref. [61]]. The results, shown in Fig. 1, are also in excellent agreement with the derived functional form.

The theory also allows us to determine the interfacial profile numerically for the analytic theta solvent case (see Supplemental Material [31] for details). Renormalizing the concentration to the infinite molecular mass limit and adjusting the constant so the center of the interface is at $x = 0$ results in Fig. 3. As one can see, the interfacial width is asymmetric. We also compare our results to those of simulations, and find them to be in qualitative agreement with the theory.

Although we recover the empirically observed molecular mass dependence, the experimental system includes both counterions and salt, both of which are ignored in our derivation thus far. We relax this constraint by updating the free energy density according to

$$f = \frac{\phi}{N}\ln\phi + g(\phi,\psi), \tag{13}$$

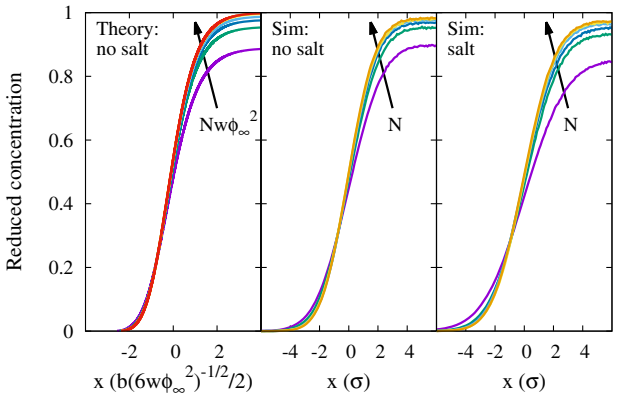

FIG. 3. Interfacial profiles normalized to infinite molecular mass for three cases: theoretically for a theta solvent with the random phase approximation expression for electrostatics (with $Nw\phi_\infty^2$ of 2, 5, 10, 20, 100, 1000, and infinity), simulations without and with salt for N ranging from 20 to 120 in increments of 20.

where ψ is the salt (and counterion) density and $g(\phi,\psi)$ includes the ideal gas contribution from salt. Two equations must be satisfied at equilibrium: (i) equality of salt chemical potential and (ii) equality of osmotic pressure in both phases. The osmotic pressure in the supernatant is no longer zero due to the presence of salt. Again, the equality of chemical potentials of the polymer is ignored, as we constrain the polymer concentration in the supernatant to be zero. A perturbative analysis yields that both ϕ and ψ should be expanded in powers of $1/N$.

The analogous interfacial tension expression [28] is

$$\gamma = 2\int_0^{\phi_c}[\kappa_\phi \Delta f]^{1/2}\left[1 + \frac{\kappa_\psi}{\kappa_\phi}\left(\frac{d\phi}{d\psi}\right)^2\right]^{1/2} d\phi, \tag{14}$$

where

$$\Delta f = f(\phi,\psi) - [\mu_\psi^{\mathrm{eq}}(\psi-\psi_c) + \mu_\phi^{\mathrm{eq}}(\phi-\phi_c) + f(\phi_c,\psi_c)]. \tag{15}$$

Subscript c denotes the coacervate phase, and μ^{eq} is the equilibrium chemical potential. These equations are supplemented by the Euler equations [$\Delta f/\partial\lambda = \kappa_\lambda(d^2\lambda/dx^2)$ with λ equal to ϕ or ψ].

The only N dependence in these equations is in Δf, ϕ_c, ψ_c. Thus, an analogous analysis can be performed to yield the same functional form of the interfacial tension with molecular mass even in the presence of salt. The only key difference is that salt has the same functional form as the polymer.

To further test our derivation, we also perform molecular dynamics simulations with explicit counterions (one small ion per charged monomer) using the same procedure as outlined above. This serves as a proxy for the addition of salt, as the counterions may now phase separate [62]. The results in Figs. 1, 2, and 3 show that the same dependencies hold. The only additional notable point is that, for the concentration of small ions in the supernatant, the first term in the expansion dominates; this is likely a direct result of the small total ion concentration.

In conclusion, we performed a comprehensive set of experiments to elucidate the molecular mass dependence of the interfacial tension far from the critical point, and proposed a theory to describe the observed scaling in the same regime. Additional validation of the theory was provided by molecular dynamics simulations.

Dr. Guangmin Wei and Dr. Anand Rahalkar (NIST) are thanked for their assistance in the preparation of qPDAMAEMA. Financial support for A. M. R. and J. J. deP. from the U.S. Department of Commerce, National Institute of Standards and Technology (NIST), through the Center for Hierarchical Materials Design (CHiMaD,70NANB14H012) is gratefully acknowledged.

*debra.audus@nist.gov
†Present address: Department of Chemical Engineering, Indian Institute of Technology Bombay, Powai, Maharashtra 400076, India.
‡Also at Center for Molecular Engineering and Materials Science Division, Argonne National Laboratory, Lemont, Illinois 60439, USA.

[1] H. G. Bungenberg de Jong, Die koazervation und ihre bedeutung für die biologie, Protoplasma **15**, 110 (1932).
[2] A. F. Thünemann, M. Müller, H. Dautzenberg, J.-F. Joanny, and H. Löwen, Polyelectrolyte Complexes, in *Advanced Computer Simulation Approaches For Soft Matter Sciences I*, Vol. 166 (Springer, Berlin, Heidelberg, 2004), pp. 113–171, https://doi.org/10.1007/b11350.
[3] J. van der Gucht, E. Spruijt, M. Lemmers, and M. A. Cohen Stuart, Polyelectrolyte complexes: Bulk phases and colloidal systems, J. Colloid Interface Sci. **361**, 407 (2011).
[4] S. Srivastava and M. V. Tirrell, Polyelectrolyte complexation, in *Advances in Chemical Physics* (John Wiley & Sons, Ltd, New York, 2016), Chap. 7, pp. 499–544, https://doi.org/10.1002/9781119290971.ch7.
[5] C. E. Sing and S. L. Perry, Recent progress in the science of complex coacervation, Soft Matter **16**, 2885 (2020).
[6] A. M. Rumyantsev, N. E. Jackson, and J. J. de Pablo, Polyelectrolyte complex coacervates: Recent developments and new frontiers, Annu. Rev. Condens. Matter Phys. **12**, 155 (2021).
[7] E. Spruijt, J. Sprakel, M. A. Cohen Stuart, and J. van der Gucht, Interfacial tension between a complex coacervate phase and its coexisting aqueous phase, Soft Matter **6**, 172 (2010).
[8] D. Priftis, R. Farina, and M. Tirrell, Interfacial energy of polypeptide complex coacervates measured via capillary adhesion, Langmuir **28**, 8721 (2012).
[9] S. Ali and V. M. Prabhu, Characterization of the ultralow interfacial tension in liquid-liquid phase separated polyelectrolyte complex coacervates by the deformed drop retraction method, Macromolecules **52**, 7495 (2019).
[10] V. M. Prabhu, Interfacial tension in polyelectrolyte systems exhibiting associative liquid-liquid phase separation, Curr. Opin. Colloid Interface Sci. **53**, 101422 (2021).
[11] R. J. Stewart, C. S. Wang, and H. Shao, Complex coacervates as a foundation for synthetic underwater adhesives, Adv. Colloid Interface Sci. **167**, 85 (2011).
[12] W. C. Blocher and S. L. Perry, Complex coacervate-based materials for biomedicine, WIREs Nanomedicine and Nanobiotechnology **9**, e1442 (2017).
[13] C. P. Brangwynne, T. J. Mitchison, and A. A. Hyman, Active liquid-like behavior of nucleoli determines their size and shape in xenopus laevis oocytes, Proc. Natl. Acad. Sci. U.S.A. **108**, 4334 (2011).
[14] E. B. Wilson, The structure of protoplasm, Science **10**, 33 (1899).
[15] T. J. Nott, E. Petsalaki, P. Farber, D. Jervis, E. Fussner, A. Plochowietz, T. D. Craggs, D. P. Bazett-Jones, T. Pawson, J. D. Forman-Kay, and A. J. Baldwin, Phase transition of a disordered nuage protein generates environmentally responsive membraneless organelles, Mol. Cell **57**, 936 (2015).
[16] Y.-H. Lin, J. D. Forman-Kay, and H. S. Chan, Sequence-Specific Polyampholyte Phase Separation in Membraneless Organelles, Phys. Rev. Lett. **117**, 178101 (2016).
[17] S. H. Anastasiadis, I. Gancarz, and J. T. Koberstein, Interfacial tension of immiscible polymer blends: Temperature and molecular weight dependence, Macromolecules **21**, 2980 (1988).
[18] E. Helfand, S. M. Bhattacharjee, and G. H. Fredrickson, Molecular weight dependence of polymer interfacial tension and concentration profile, J. Chem. Phys. **91**, 7200 (1989).
[19] D. Broseta, G. H. Fredrickson, E. Helfand, and L. Leibler, Molecular weight and polydispersity effects at polymer-polymer interfaces, Macromolecules **23**, 132 (1990).
[20] H. Tang and K. F. Freed, Interfacial studies of incompressible binary blends, J. Chem. Phys. **94**, 6307 (1991).
[21] A. V. Ermoshkin and A. N. Semenov, Interfacial tension in binary polymer mixtures, Macromolecules **29**, 6294 (1996).
[22] A. Semenov, Theory of long-range interactions in polymer systems, J. Phys. II **6**, 1759 (1996).
[23] R. A. Riggleman, R. Kumar, and G. H. Fredrickson, Investigation of the interfacial tension of complex coacervates using field-theoretic simulations, J. Chem. Phys. **136**, 024903 (2012).
[24] T. K. Lytle, A. J. Salazar, and C. E. Sing, Interfacial properties of polymeric complex coacervates from simulation and theory, J. Chem. Phys. **149**, 163315 (2018).
[25] J. Qin, D. Priftis, R. Farina, S. L. Perry, L. Leon, J. Whitmer, K. Hoffmann, M. Tirrell, and J. J. de Pablo, Interfacial tension of polyelectrolyte complex coacervate phases, ACS Macro Lett. **3**, 565 (2014).
[26] J. T. G. Overbeek and M. J. Voorn, Phase separation in polyelectrolyte solutions. theory of complex coacervation, J. Cell. Comp. Physiol. **49**, 7 (1957).
[27] Voorn-Overbeek is a combination of Flory-Huggins theory to treat the non-electrostatic interactions and Debye-Hückel theory to treat the electrostatic interactions.
[28] J. W. Cahn and J. E. Hilliard, Free Energy of a Nonuniform System. I. Interfacial Free Energy, J. Chem. Phys. **28**, 258 (1958).
[29] H. Shao and R. J. Stewart, Biomimetic underwater adhesives with environmentally triggered setting mechanisms, Adv. Mater. **22**, 729 (2010).
[30] Degree of quaternization was greater or equal to 98%; see Supplemental Material [31].
[31] See Supplemental Material at http://link.aps.org/supplemental/10.1103/PhysRevLett.126.237801 for a detailed description of experimental procedures including materials, sample preparation, polymer concentration measurements, rheological measurements, and interfacial tension measurements, as well as the details of the interfacial tension derivation, scaling estimates for h, and interfacial profile calculation, which includes Refs. [9,19,32–36].
[32] E. Spruijt, M. A. Cohen Stuart, and J. van der Gucht, Linear viscoelasticity of polyelectrolyte complex coacervates, Macromolecules **46**, 1633 (2013).
[33] P. K. Jha, P. S. Desai, J. Li, and R. G. Larson, pH and salt effects on the associative phase separation of oppositely charged polyelectrolytes, Polymers **6**, 1414 (2014).

[34] Y. Ma, S. Ali, and V. M. Prabhu, Pseudo-Binodal Phase Diagram and Concentration Fluctuations in Aqueous Polyelectrolyte Complexes, (to be published).
[35] H. Mo, C. Zhou, and W. Yu, A new method to determine interfacial tension from the retraction of ellipsoidal drops, J. Non-Newtonian Fluid Mech. **91**, 221 (2000).
[36] P. de Gennes, *Scaling Concepts in Polymer Physics* (Cornell University Press, Ithaca, 1979).
[37] S. Ali, M. Bleuel, and V. M. Prabhu, Lower critical solution temperature in polyelectrolyte complex coacervates, ACS Macro Lett. **8**, 289 (2019).
[38] V. Y. Borue and I. Y. Erukhimovich, A statistical theory of globular polyelectrolyte complexes, Macromolecules **23**, 3625 (1990).
[39] J. Qin and J. J. de Pablo, Criticality and connectivity in macromolecular charge complexation, Macromolecules **49**, 8789 (2016).
[40] A. Salehi and R. G. Larson, A molecular thermodynamic model of complexation in mixtures of oppositely charged polyelectrolytes with explicit account of charge association/dissociation, Macromolecules **49**, 9706 (2016).
[41] K. T. Delaney and G. H. Fredrickson, Theory of polyelectrolyte complexation–complex coacervates are self-coacervates, J. Chem. Phys. **146**, 224902 (2017).
[42] G. H. Fredrickson, *The Equilibrium Theory of Inhomogeneous Polymers* (Oxford University Press, Oxford, 2006).
[43] P. J. Flory, *Principles of Polymer Chemistry* (Cornell University Press, Ithaca, 1953).
[44] Technically, these theories have interaction potentials that are N independent. One can also have N contributions from end effects as considered in Refs. [21,22] for the neutral system case; the result is a modified numerical prefactor for h.
[45] E. Spruijt, A. H. Westphal, J. W. Borst, M. A. Cohen Stuart, and J. van der Gucht, Binodal compositions of polyelectrolyte complexes, Macromolecules **43**, 6476 (2010).
[46] L. Li, S. Srivastava, M. Andreev, A. B. Marciel, J. J. de Pablo, and M. V. Tirrell, Phase behavior and salt partitioning in polyelectrolyte complex coacervates, Macromolecules **51**, 2988 (2018).
[47] A. M. Rumyantsev, E. B. Zhulina, and O. V. Borisov, Complex coacervate of weakly charged polyelectrolytes: Diagram of states, Macromolecules **51**, 3788 (2018).
[48] E. J. Hinch, *Perturbation Methods*, Cambridge Texts in Applied Mathematics (Cambridge University Press, Cambridge, England, 1991).
[49] N. N. Oskolkov and I. I. Potemkin, Complexation in asymmetric solutions of oppositely charged polyelectrolytes: Phase diagram, Macromolecules **40**, 8423 (2007).
[50] A. S. Bodrova, E. Y. Kramarenko, and I. I. Potemkin, Microphase separation induced by complexation of ionic-non-ionic diblock copolymers with oppositely charged linear chains, Macromolecules **43**, 2622 (2010).
[51] A. M. Rumyantsev and I. I. Potemkin, Explicit description of complexation between oppositely charged polyelectrolytes as an advantage of the random phase approximation over the scaling approach, Phys. Chem. Chem. Phys. **19**, 27580 (2017).
[52] M. Rubinstein, Q. Liao, and S. Panyukov, Structure of liquid coacervates formed by oppositely charged polyelectrolytes, Macromolecules **51**, 9572 (2018).
[53] U. Micka, C. Holm, and K. Kremer, Strongly charged, flexible polyelectrolytes in poor solvents: Molecular dynamics simulations, Langmuir **15**, 4033 (1999).
[54] Z. Wang and M. Rubinstein, Regimes of conformational transitions of a diblock polyampholyte, Macromolecules **39**, 5897 (2006).
[55] S. Plimpton, Fast parallel algorithms for short-range molecular dynamics, J. Comput. Phys. **117**, 1 (1995).
[56] Large-scale atomic/molecular massively parallel simulator, http://lammps.sandia.gov, accessed: December 2019.
[57] R. J. Roe, SAXS study of micelle formation in mixtures of butadiene homopolymer and styrene-butadiene block copolymer. 3. comparison with theory, Macromolecules **19**, 728 (1986).
[58] A. Y. Grosberg and A. R. Khokhlov, *Statistical Physics of Macromolecules* (AIP Press, New York, 1994).
[59] Technically as pointed out in Ref. [60], the expression for f is not the same as in Eq. (2), but the final functional form of the results is unchanged as the correct form of f is also an expansion in powers of $1/N$.
[60] X. C. Zeng, D. W. Oxtoby, H. Tang, and K. F. Freed, On squaregradient theories of polymer blend interfaces, J. Chem. Phys. **96**, 4816 (1992).
[61] G. J. Gloor, G. Jackson, F. J. Blas, and E. de Miguel, Test-area simulation method for the direct determination of the interfacial tension of systems with continuous or discontinuous potentials, J. Chem. Phys. **123**, 134703 (2005).
[62] For the simulated system with counterions, there exists a thermodynamically equivalent one where the supernatant has a larger total volume but additional salt is added such that the concentrations are unchanged.